PHYSICAL REVIEW C

NUCLEAR PHYSICS

THIRD SERIES, VOLUME 37, NUMBER 6 JUNE 1988

Giant $E1$ resonances in ^{20}Ne observed with the ^{19}F($\vec{p},\gamma_0\gamma_1$)^{20}Ne reactions

P. M. Kurjan,* J. R. Calarco,† G. A. Fisher,‡ and S. S. Hanna
Department of Physics, Stanford University, Stanford, California 94305
(Received 25 June 1987)

The giant electric dipole resonance built upon the 0^+ ground state of ^{20}Ne was studied via the ^{19}F($\vec{p},\gamma_0$)^{20}Ne reaction. Polarized and unpolarized angular distributions were measured between $E_x = 16.1$ and 23.0 MeV ($E_p = 3-10$ MeV) and the $E1$ T-matrix elements extracted. The ^1P, $E1$ partial wave dominates, but the weaker ^3P (spin flip) term is also resonant. A heuristic doorway state model has been used to fit the pronounced structure in the giant $E1$ resonance. Data for the giant resonance built on the first excited state as seen in the ^{19}F($\vec{p},\gamma_1$)^{20}Ne reaction are presented and discussed. The microscopic, doorway state calculation in a deformed potential of Schmid and Do Dang is in very good agreement with the main features of the results.

I. INTRODUCTION

The giant electric dipole resonance (GDR) has been extensively studied in nuclear physics.[1] Because of its well-defined systematics, such as large integrated cross section typically about 60NZ/A mb MeV, width on the order of 3–5 MeV, centroid varying as $80A^{-1/3}$ MeV, and similar angular distributions of decay products, it has also lent itself to extensive theoretical treatment.[2] Natural candidates for these studies are the (γ,x) reactions with (γ,p) and specifically (γ,p_0) providing important results. By time reversal invariance (detailed balance), the latter reaction is equivalent to the (p,γ_0) process; in fact, many of the possible (p,γ_0) reactions leading to giant resonances in the compound nucleus have been studied experimentally. The earlier studies with unpolarized protons were subsequently extended with the use of polarized protons.[3]

Studies of the $4N$ nuclei, with their desirable shell characteristics and often simple angular momentum couplings, have proven to be especially meaningful. The case of ^{20}Ne, first studied through ^{19}F($p,\gamma_0\gamma_1$)^{20}Ne by Segel *et al.*,[4] is of particular interest because of the pronounced intermediate structure displayed by the giant $E1$ resonances built on the ground and first excited states. The (p,γ_0) angular distributions showed the constancy over the intermediate structure that is typical of giant resonances, which suggests a constant or similar particle-hole configuration for all the structure. Yet, an *ad hoc* fit of four distinct Breit-Wigner resonances to the cross section data proved quite successful.[5] The γ-ray transitions to the 0^+ ground state of ^{20}Ne may originate from 1^-, 1^+, and 2^+ compound states, giving γ-ray multipolarities of $E1$, $M1$, and $E2$, respectively. Higher multipolarities ($M2, E3, \ldots,$) are very weak in the region studied and may be neglected. Ample evidence[6] suggests that most of the $M1$ strength in ^{20}Ne is found below the region of the GDR, principally in the well-known level at 11.4 MeV. Thus, it might be possible to analyze the data in the present experiment on the assumption that only $E1$ and $E2$ radiations are present. In a companion paper[7] we note that this assumption produced excellent fits to precise angular distribution data except in a narrow region around $E_x = 18$ MeV in ^{20}Ne. This difficulty was attributed to the presence of $M1$ radiation. However, in the present analysis which seeks only the $E1$ strength, the assumption of $E1$ and $E2$ radiation is justified.

For the ^{19}F(p,γ_0)^{20} reaction, the proton channels leading to $E1$ and $E2$ radiations each involve two partial waves yielding a total of seven quantities (four amplitudes and three phase differences) that must be determined for a complete description of the reaction. The unpolarized angular distribution measurements yield only five experimental quantities if enough angles are measured so that in the expansion

$$\sigma(E,\theta) = A_0(E)[1 + \Sigma a_k(E) P_k(\cos\theta)]$$

the total cross section $4\pi A_0$ and the four Legendre coefficients through the term in P_4 can be determined. The availability of polarized protons, however, allows angular distribution measurements of analyzing powers $A(E,\theta)$ to be made which give four additional experimental parameters, the four associated Legendre coefficients through the term in P_4 in the expansion

$$A(E,\theta)\sigma(E,\theta) = A_0(E)\Sigma b_k(E) P_k^1(\cos\theta) .$$

Thus, there are now nine experimental quantities that can be used to (over)determine the seven unknown amplitudes and phases. As a result, γ-ray angular distribution measurements of sufficient precision using both polarized and unpolarized protons allow a complete determination of the proton partial wave configurations leading to the emission of $E1$ and $E2$ radiations.

Since the thrust of the present work was to obtain information on the GDR of ^{20}Ne, the extraction of $E2$ strength was not stressed, and only three angles were measured in the polarized angular distributions. These were chosen so as to maximize the sensitivity to $E1$ radiation at the expense of $E2$ radiation. This limitation on the number of angles reduces the number of independent experimental quantities from nine to eight, which are still enough to determine all the amplitudes and phases.

II. EXPERIMENTAL METHOD

Polarized protons obtained from an ANAC ground state atomic beam type of source[8] were accelerated by the Stanford FN tandem accelerator, and the γ rays from the reactions ^{19}F(p;γ_0,γ_1)^{20}Ne, $Q=12.845$, 11.211 MeV were detected by the Stanford 25×25 cm NaI spectrometer equipped with an anticoincidence shield.[9] The target was a layer of CaF_2 deposited on thin gold foils. The beam polarization was measured periodically with the well studied ^{12}C(p,p$_0$) reaction[10] at $E_p=9.8$ MeV and $\theta=70°$, and monitored continuously by recording the elastically scattered protons from ^{19}F(p,p$_0$) at $\theta=30°$ on the side of the reaction opposite the γ spectrometer.

A typical ^{19}F(p,γ) spectrum is shown in Fig. 1. The well-resolved (in all spectra) transitions to the ground and first excited states of ^{20}Ne (γ_0 and γ_1) were fitted by a computer with standard line shapes obtained from reactions such as ^{11}B(p,γ_0) and ^{15}N(p,γ_0). These reactions provide isolated peaks with energies that bracket the region of interest in ^{20}Ne. The large background below 10 MeV in Fig. 1 is due mostly to thermal neutron capture γ rays in Fe, and to the bountiful ^{19}F(p,α,γ) reaction. In this region, into which the γ_0 and γ_1 fits cannot be extended, the line shapes were extrapolated linearly to zero at $E_\gamma=0$. We estimate the absolute error in this procedure at less than 10% and, presumably, it does not introduce any relative errors into the results.

The 90° yield curves for γ_0 and γ_1 (Fig. 2), obtained from fairly thick targets (typically 2 mg/cm^2 of CaF_2), agree with the results of Segel *et al.*[4] but do not display all the fine structure seen in these thinner target measurements. The (p,γ) results also agree well with the (γ,n) (Ref. 11) and (e,e') (Ref. 12) experiments. A curious feature of these data is the apparent strong correlation between the γ_0 and γ_1 yields, as will be discussed herein.

Seven-angle (between 40° and 140°) unpolarized distributions and three-angle (45°, 90°, and 135°) polarized distributions were obtained separately but systematically throughout the region of the GDR. Some typical distri-

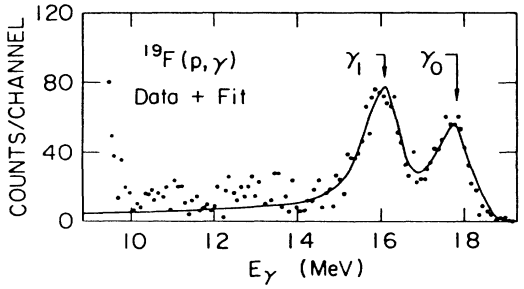

FIG. 1. Typical spectrum for the ^{19}F(p,γ)^{20}Ne reaction. The two-line-shape fit is superimposed on the data.

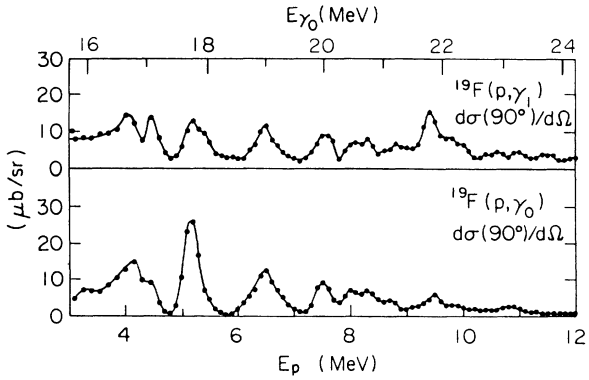

FIG. 2. The 90° yield curves for the ^{19}F(p,γ_0)^{20}Ne and ^{19}F(p,γ_1)^{20}Ne* reactions. The curves are drawn merely to guide the eye.

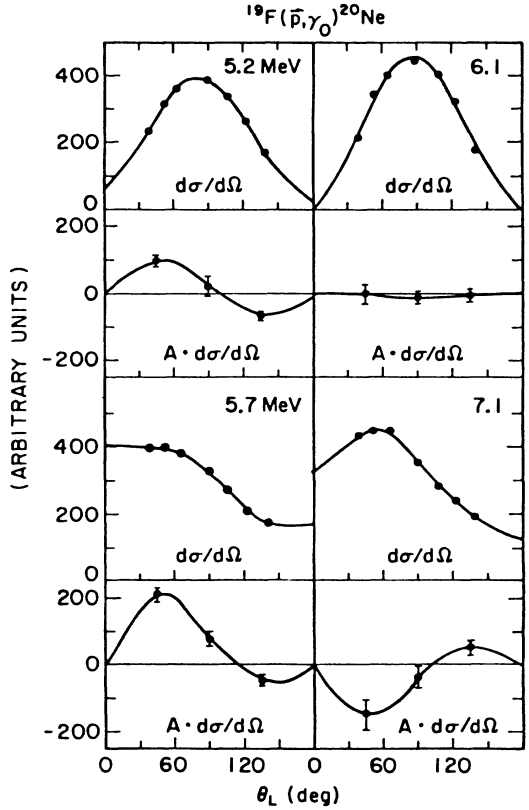

FIG. 3. A sample of the unpolarized and polarized angular distributions for the ^{19}F(p,γ_0)^{20}Ne reaction. The proton bombarding energy is given for each pair of curves.

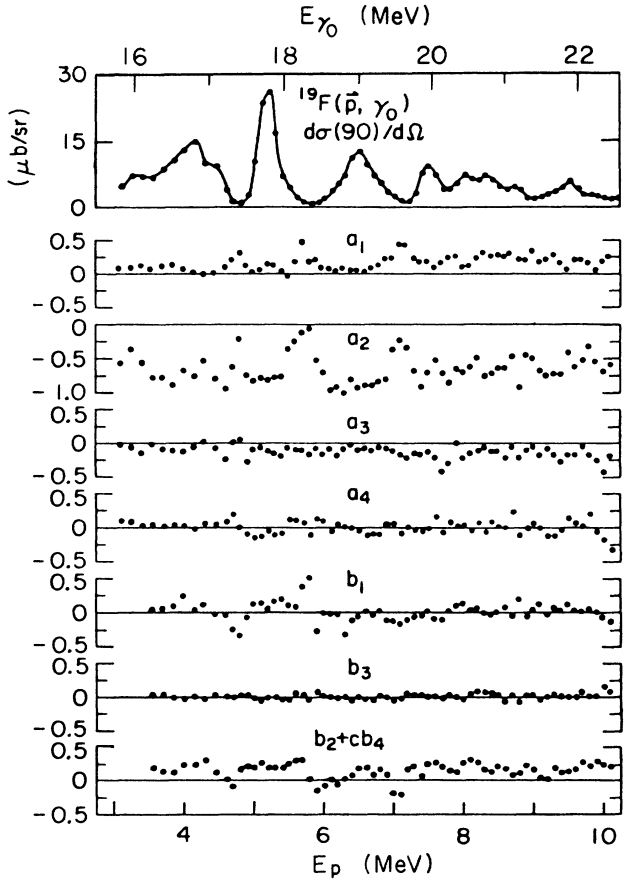

FIG. 4. The angular distribution yield coefficients and analyzing power coefficients derived from the ^{19}F(p,γ_0)^{20}Ne measurements. The values of b_1, b_3, and the linear combination $b_2+0.41b_4$ are extracted from three-point angular distributions at 45°, 90°, and 135°.

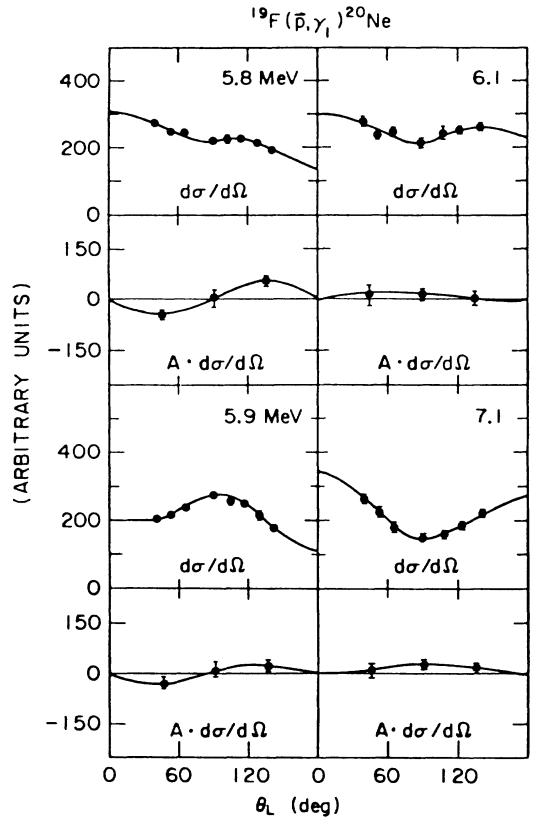

FIG. 5. A sample of the unpolarized angular distributions for the ^{19}F(p,γ_1)^{20}Ne reaction. The proton bombarding energy is given for each pair of curves.

butions for γ_0 are shown in Fig. 3. All the Legendre and associated coefficients extracted from the γ_0 distributions are shown in Fig. 4. The overall constancy of these coefficients (distributions) is apparent, although there are notable fluctuations in the valleys of the cross section curve. The nonzero, positive values of a_1 indicate the presence of radiation of parity opposite to $E1$, presumably chiefly $E2$ radiation. The fairly constant, small, negative values of a_3 are a clear signature for interfering radiation of multipolarity greater than unity, i.e., $E2$ radiation. Some typical angular distributions for γ_1, both unpolarized and polarized, are shown in Fig. 5, and all the extracted Legendre coefficients are presented in Fig. 6.

III. THE GROUND STATE GDR

We now proceed to analyze the γ_0 results in terms of $E1$ and $E2$ transitions. For ^{20}Ne, a light nucleus removed from a closed shell, we choose to work in the LS coupling scheme. This choice is arbitrary in that the actual configuration can be constructed either from the LS or the jj configurations. In this coupling scheme the proton partial waves are ^1P and ^3P for formation of a 1^- state leading to $E1$ radiation and ^1D and ^3D for a 2^+ state and $E2$ radiation. We designate the amplitudes of these partial waves by $|\,^1P\,|$, $|\,^3P\,|$, $|\,^1D\,|$, and $|\,^3D\,|$, and their relative phase differences by (^1P,^3P), (^1P,^1D), and (^1P,^3D), where (^1P,^3P) is shorthand for $\phi(^1P)-\phi(^3P)$, etc. The relationships between the angular distribution coefficients and the partial waves then turn out to be[5]

$$
\begin{aligned}
\sigma &= |\,^1P\,|^2+|\,^3P\,|^2+|\,^1D\,|^2+|\,^3D\,|^2\,,\\
\sigma a_1 &= 2.683\,|\,^1P\,|\,|\,^1D\,|\cos(^1P,^1D)\\
&\quad +2.324\,|\,^3P\,|\,|\,^3D\,|\cos(^3P,^3D)\,,\\
\sigma a_2 &= -|\,^1P\,|^2+0.5\,|\,^3P\,|^2\\
&\quad +0.7143\,|\,^1D\,|^2+0.3571\,|\,^3D\,|^2\,,\\
\sigma a_3 &= -2.683\,|\,^1P\,|\,|\,^1D\,|\cos(^1P,^1D)\\
&\quad +1.549\,|\,^3P\,|\,|\,^3D\,|\cos(^3P,^3D)\,,\\
\sigma a_4 &= -1.714\,|\,^1D\,|^2+1.143\,|\,^3D\,|^2\,,\\
\sigma b_1 &= 1.643\,|\,^1P\,|\,|\,^3D\,|\sin(^1P,^3D)\\
&\quad +0.949\,|\,^3P\,|\,|\,^1D\,|\sin(^3P,^1D)\,,\\
\sigma b_3 &= -0.730\,|\,^1P\,|\,|\,^3D\,|\sin(^1P,^3D)\\
&\quad +0.633\,|\,^3P\,|\,|\,^1D\,|\sin(^3P,^1D)\,,\\
\sigma[b_2+c(\xi)b_4] &= 0.707\,|\,^1P\,|\,|\,^3P\,|\sin(^1P,^3P)\,,
\end{aligned}
\tag{1}
$$

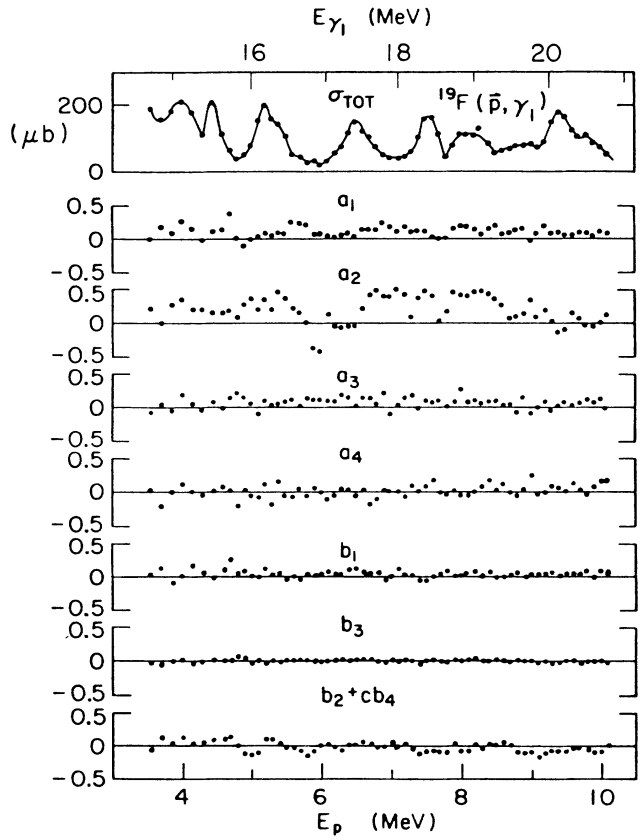

FIG. 6. The angular distribution yield coefficients and analyzing power coefficients derived from the $^{19}F(p,\gamma_1)^{20}Ne^*$ measurements. The values of b_1, b_3, and the linear combination $b_2+0.41b_4$ are extracted from three-point angular distributions at 45°, 90°, and 135°. At the top is the total cross section curve.

as derived for a complete yield angular distribution (number of angles greater than four) but an analyzing power distribution restricted to the three angles ξ, 90°, and $180°-\xi$. We note that the nature of this restriction leads to a measurement of the linear combination $b_2+c(\xi)b_4$ which depends only on the dipole partial waves ^1P and ^3P. The parameter

$$c(\xi)=P_4(\cos\xi)/p_2(\cos\xi)\ .$$

In this experiment $\xi=45°$ and $c(45°)=0.417$. It is this simplification in the data taking that deemphasizes the measurement of the $E2$ radiation.

For pure $E1$ radiation, i.e., no $E2$ radiation, these relations (1) collapse to

$$\begin{aligned}\sigma &= |\,^1P\,|^2+|\,^3P\,|^2\ ,\\ \sigma a_2 &= -1.0\,|\,^1P\,|^2+0.5\,|\,^3P\,|^2\ ,\\ \sigma b_2 &= 0.707\,|\,^1P\,|\,|\,^3P\,|\sin(^1P,^3P)\ .\end{aligned}\tag{2}$$

Thus, for pure $E1$

(a) only the coefficients a_2 and b_2 are nonzero;

(b) only a_2 is nonzero if only one partial wave contributes to $E1$ (a polarization effect requires interference);

(c) if the partial wave is ^1P then $a_2=-1.0$;

(d) if it is the spin-flip configuration ^3P then $a_2=+0.5$.

For $E1$ radiation we expect the non-spin-flip to dominate the spin-flip transitions. In fact, the "constant" value of a_2 (see Fig. 4) of about -0.8 in the structure peaks is strong preliminary evidence that the expected ^1P configuration is indeed dominant in the ground state GDR of ^{20}Ne.

The solutions to Eqs. (2), the pure $E1$ case, can be presented graphically as is done in Fig. 7, where the total cross section $\sigma=4\pi A_0$ is normalized to unity. Because of the quadratic nature of the equations, for each value of a_2 and of b_2 there are two solutions, given by the two points where the horizontal line corresponding to the value of a_2 intersects the closed curve corresponding to the value of b_2. Because of the choice of LS coupling scheme which leads to horizontal lines for values of a_2 corresponding to single values of $|\,^1P\,|^2$, the two solutions have identical values for the two intensities $|\,^1P\,|^2$ and $|\,^3P\,|^2$ but two separate, symmetric values for the phase difference $(^1P,^3P)=\eta$ and $180°-\eta$. Thus in pure LS coupling there is no ambiguity with respect to the strength of non-spin-flip versus spin-flip transitions. if we adopt values of $a_2=-0.8$ and $b_2=0.2$ over the peaks in the GDR, the two solutions (from Fig. 7) are $|\,^1P\,|^2=0.87$, $|\,^3P\,|^2=0.13$ and $(^1P,^3P)=55°$ or 125°, indicating, as above, a dominant non-spin-flip component.

The detailed analysis of the data could now be carried out by using the complete Eqs. (1) for $E1$ and $E2$ radiations. In actual fact the final analysis was not done in a two-step procedure by going from the experimental data to the Legendre coefficients to the partial wave amplitudes and phases, but in a single step process from the experimental data directly to the amplitudes and phases. In this latter procedure it is easier to propagate the experimental uncertainties into correct errors in the final results. These results are displayed in Fig. 8. We do not show the results for the ^1D and ^3D partial waves which lead to $E2$ radiation. They are small at all energies and were determined with low precision since only three-point polarization distributions were obtained.

It is apparent in Fig. 8 that the ^1P dominates the ^3P partial wave throughout and that both resonate with the intermediate structure in the total cross section. This is further evidence of the remarkable and dominant characteristic of the GDR that, no matter how complex and pronounced the structure, a fairly constant angular distribution seems to be impressed over the whole GDR even though the microscopic configuration might be changing drastically.[1] Some success has been achieved in explaining this feature by a doorway-state model as discussed herein. Only one of the two choices for the phase difference $(^3P,^1P)$ is plotted in Fig. 5. We see that fluctuations in the phases also seem to correlate with the valleys of the structure.

Figure 8 also shows the total cross sections for $E1$ and $E2$ strength in the region studied, as obtained from the $^1P,^3P$ and $^1D,^3D$ amplitudes, respectively. Although plotted to a larger scale, it is readily apparent that the $E2$ strength is much smaller and not determined with great

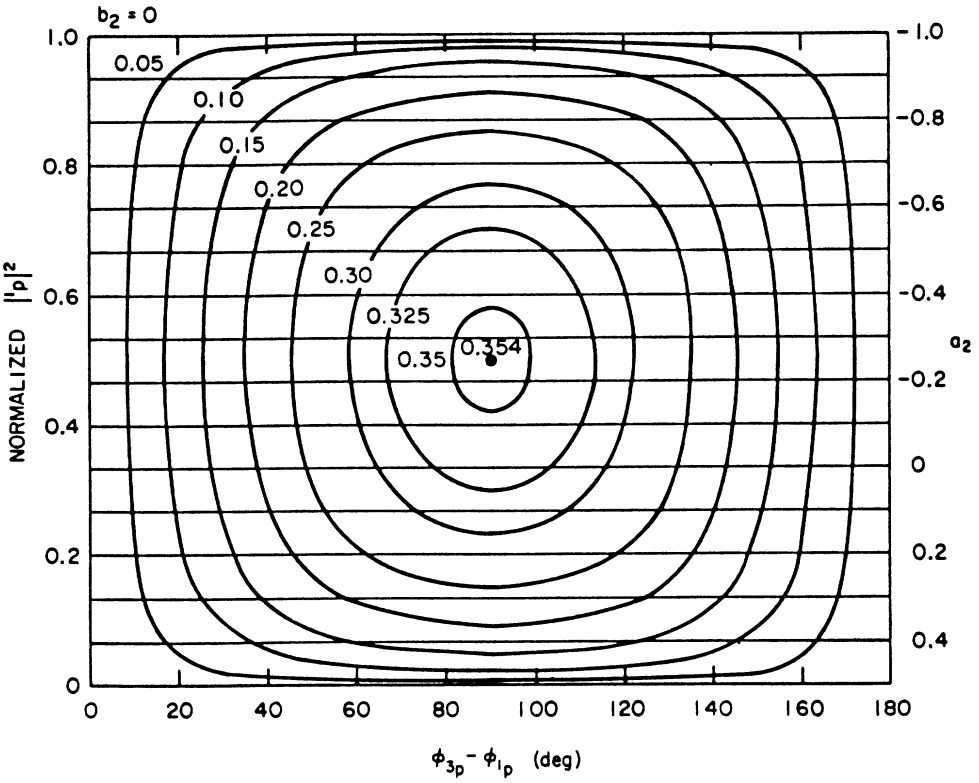

FIG. 7. Possible solutions of Eq. (2) normalized to $\sigma = 4\pi A_0 = 1$. The intersections of the horizontal a_2 lines and b_2 closed curves give the possible solutions (see the text). This diagram is valid for any capture reaction with the spin sequence $\frac{1}{2}^+(\frac{1}{2}^+,\gamma)0^+$ as for ^{19}F(p,γ_0)^{20}Ne.

precision. The $E2$ strength has now been measured with much better precision in the companion paper[7] and is discussed there.

If the total $E1$ capture cross sections are converted to cross sections for the inverse ^{20}Ne(γ,p_0)^{19}F reaction by detailed balance and then integrated over the region of observation ($E_\gamma = 15.5$–23 MeV), it is found that 8.5% of the electric dipole sum rule (60 NZ/A mb MeV) is exhausted by the p_0 decay channel in the photoexcitation of the GDR of ^{20}Ne. This is a fairly typical value for the light nuclei.

IV. THE FIRST EXCITED STATE GDR

The properties of the giant resonance built upon the first excited state of ^{20}Ne (we adopt the notation GDR_1 and GDR_0 for the first excited and the ground state GDR's) as studied by the ^{19}F(p,γ_1)^{20}Ne* reaction can be seen in Figs. 2, 5, and 6. Because of the pronounced structure in both GDR_1 and GDR_0, it is difficult to see if the center of GDR_1 is shifted up from that of GDR_0 by the excitation energy of the first excited state (1.63 MeV) as is observed in many other cases.[13] To test this point the centroids of both distributions were computed. In both cases a γ ray interval from 15.66 to 21.25 MeV was used. For GDR_0 the centroid comes at a γ energy of 18.2 MeV, whereas for GDR_1 it lies at 18.6 MeV. Thus, to the extent that the strengths are localized, the excitation energy of GDR_1 based on the first excited state is, if anything, greater than the energy of GDR_0.

If the total cross section curve for γ_1 (Fig. 6) is converted to a curve for ^{20}Ne*(γp_0)^{19}F by detailed balance, the integrated $E1$ strength over the region studied is found to be about 3.5% of the dipole sum rule after subtraction of a nominal $E2$ strength of $\approx$3.0%. That this $E1$ strength is only $\approx$40% that of the p_0 channel for GDR_0 can be traced to the fact that the (p,γ_1) strength is not $2J+1=5$ times stronger than the (p,γ_0) strength as observed in other cases in the light nuclei.[14] This in turn may be due to the fact that GDR_1 is more spread out than GDR_0 and strength is thereby missing from GDR_1, or simply that the microscopic configuration of GDR_1 is less likely to decay into the p_0 channel than is the configuration of GDR_0.

Another feature of GDR_1 is the apparent presence of structure strongly correlated with the GDR_0 structure. Since such a correlation is not expected, we have carried out a cross-correlation analysis[13] between the two yield curves in Fig. 2. The large amplitudes of the correlation curves, shown in Fig. 9, reveal a significant degree of correlation. Such a result would imply that the 1^- structures in GDR_0 also contribute significantly to GDR_1, although there is no *a priori* reason for this to be so. No other such case has been observed. We note that the possible deformation of the ^{20}Ne nucleus does not appear to

be the cause of this correlation (see the following).

In GDR_1 there can be 1^-, 2^-, and 3^- states that connect to the 2^+ first excited state by $E1$ radiation, 0^+, 1^+, 2^+, 3^+, and 4^+ states that go by $E2$ radiation, and 1^+, 2^+, and 3^+ states that decay by $M1$ radiation. Thus, a complete analysis in terms of $E1$, $E2$, and $M1$ radiation would require determination of 43 parameters (22 partial wave amplitudes and 21 relative phase differences). The $M1$ radiation is included since there is little information about the location of $M1$ strength based on the first excited state. Thus, it is quite impossible to obtain enough experimental information to determine all these parameters. Even if it was desired to study the case of pure $E1$ radiation, the complexity would be prohibitive. In view of these difficulties we choose to wait for theoretical guidance before attempting an analysis of GDR_1.

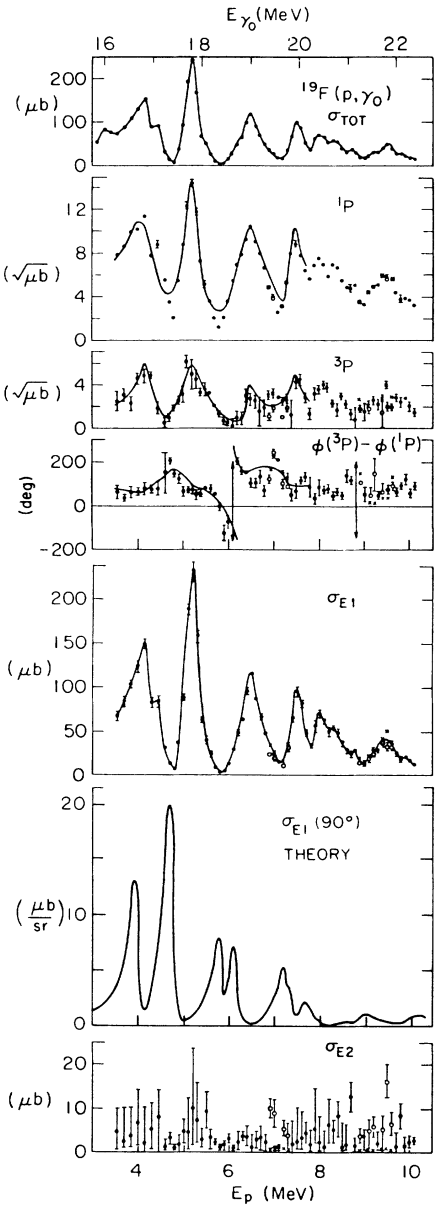

FIG. 8. The $E1$ partial wave amplitudes, ^1P and ^3P, and relative phase for the $^{19}F(p,\gamma_0)^{20}Ne$ reaction extracted from the angular distribution measurements. The solid lines superimposed on these data are fits discussed in the text.[5] The total $E1$ and $E2$ cross sections derived from the ^1P, ^3P and ^1D, ^3D (not shown) amplitudes, respectively, are labeled σ_{E1} and σ_{E2}, respectively. The curve through the $E1$ data is drawn merely to guide the eye. The 90° differential cross section curve labeled THEORY is derived in Ref. 23 as discussed in the text. At the top is given the total cross section curve.

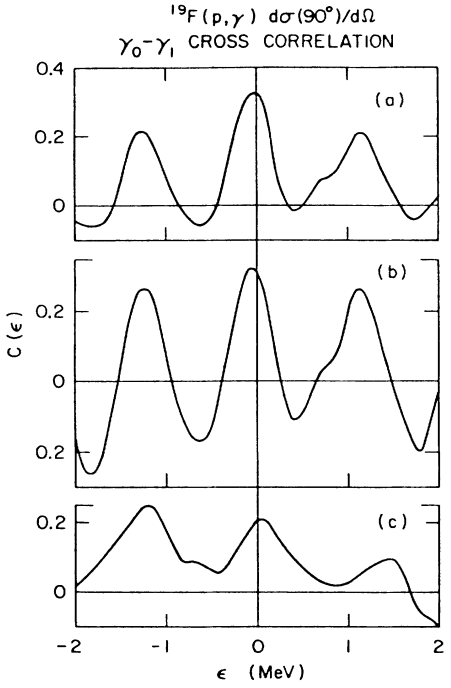

FIG. 9. The cross-correlation coefficient calculated between the 90° yield curves of γ_0 and γ_1. The significance and notation of cross-correlation functions are discussed in Ref. 13. The calculation over the whole region from $E_p = 3.6$ to 12.0 MeV is in (a), over the partial region from 3.6 to 8.0 MeV in (b), and from 8.1 to 12.0 MeV in (c).

V. THE DOORWAY STATE MODEL

The doorway-state model of nuclear reactions[15] has been used to explain the appearance of structure of intermediate width in reaction cross section curves. In the formation of a giant resonance, the width of the intermediate structure lies between that of the overall giant resonance (gross structure) and the average width of the statistical (Ericson) fluctuations (fine structure). An outstanding case is that of the GDR's in ^{28}Si as revealed by the $^{27}Al(p,\gamma_0\gamma_1)^{28}Si$ reactions.[13] The doorway model has been applied with considerable success,[16,17] to explain the structure that appears in the GDR of ^{16}O. In this case the main GDR may consist of two gross structures which are then broken up into several intermediate structures that may be associated with resonances in decay channels other than the proton channel.[18–20] No fine structure has been identified[21] with any certainty in ^{16}O, as is reasonable from a consideration of the coherence width

in such a light nucleus.

The GDR's in ^{20}Ne as displayed by the ^{19}F(p,$\gamma_0\gamma_1$)^{20}Ne reactions would appear to be extreme cases of intermediate structure, in that the GDR strength appears to be broken up almost entirely into such structures. This idea has been tested in an *ad hoc* manner by assuming the main GDR strength built on the ground state lies in four coherent intermediate states of Breit-Wigner shape. The principal results of the analysis have been published elsewhere,[5] but in Fig. 8 we show the fits achieved to the amplitudes and phases.

In an important series of papers, Schmid and Do Dang[22] have given a fully microscopic treatment of the proton capture process especially as it applies to the ^{19}F(p,$\gamma_0\gamma_1$)^{20}Ne reactions. The calculation is based on the Feshbach formulism incorporating the doorway state description[15] as later applied to ^{16}O by Shakin and Wang.[16] The bound states are described as linear combinations of angular momentum projected 1p-1h configurations in a deformed Hartree-Fock basis. Thus, we can think of the calculation as a microscopic doorway state model in a deformed potential which gives rise naturally to the type of pronounced intermediate structure that is seen in both the γ_0 and γ_1 yield curves. Schmid and Do Dang[22] illustrate direct comparisons between the theoretical and experimental yield curves. For γ_0 the theory faithfully and strikingly reproduces the observed intermediate structures in considerable detail, although some shifts in energy are apparent. (See Fig. 8.) For γ_1 the same kind of pronounced structure is obtained but a one-to-one correspondence with experiment is not apparent. For the angular distributions some success is achieved in reproducing the dominant $E1$ features as portrayed by the a_2 coefficient of the distributions. In general more fluctuations in the a_2 curves are found theoretically than are observed experimentally, a common failure of theory calculations.[23] For the other coefficients (a_1, a_3, and a_4) less success is obtained, but here the difficulty may be attributed more to the treatment of the multipoles other than $E1$. As yet the calculations have not been used to obtain a comparison with the partial wave amplitudes and phases found experimentally. In summary, we believe the work of Schmid and Do Dang, coupled with the success of the earlier work on ^{16}O, provides very strong support for the doorway state model.

VI. CONCLUSIONS

In this study of the ^{19}F(p,γ_0)^{20}Ne reaction we find that $E1$ radiation is dominant over the $E2$ contribution, if it is assumed that nearly all the $M1$ radiation is concentrated in the level at 11.4 MeV. The use of polarized protons enables all the $E1$ and $E2$ partial waves and phase differences to be determined. Both the ^1P and ^3P partial waves resonate with the intermediate structure, but the spin-flip ^3P wave is much weaker as expected for $E1$ radiation.

The microscopic deformed doorway state calculations of Schmid and Do Dang are in good qualitative agreement with the experimental yield curves but are not able to fit the angular distribution data as well. The $E1$ partial wave amplitudes and phases are not yet available from such calculations. It is noted that a good fit can be made to the amplitudes and phases with four partially overlapping Breit-Wigner resonances.

The yield curves for γ_0 and γ_1 both display pronounced intermediate structure in agreement with earlier results. The γ_1 structures correlate strongly with those of γ_0, suggesting that γ_1 decays originate from some of the same intermediate states with $J^\pi = 1^-$. Because of the possible presence of GDR$_1$ states with $J^\pi = 1^-$, 2^-, 3^-, 0^+, 1^+, 2^+, 3^+, and 4^+, the γ_1 angular distribution data cannot produce an exact solution for all of the possible partial waves which would allow a test of this hypothesis. Similar strong correlations are not apparent in the work of Schmid and Do Dang.

We are grateful to the National Science Foundation for partial support of this research.

---

*Present address: Consilium Associates Inc., 1945 Charleston Rd., Mountain View, CA 94043.

†Present address: Department of Physics, University of New Hampshire, Durham, NH 03824.

‡Present address: Department of Physics, San Francisco State University, San Francisco, CA 94132.

[1]S. S. Hanna, in *Photonuclear Reactions I,* Vol. 61 of *Lecture Notes in Physics,* edited by S. Costa and C. Schaerf (Springer-Verlag, Berlin, 1976), p. 275.

[2]G. E. Brown, *Unified Theory of Nuclear Models* (North-Holland, Amsterdam, 1964).

[3]S. S. Hanna, in *Nuclear Structure Studies Using Electron Scattering and Phooreaction,* edited by K. Shoda and H. Ui (Tomizawa, Sendai, Japan, 1972), p. 453.

[4]R. E. Segel, Z. Vager, L. Meyer-Schützmeister, P. P. Singh, and R. G. Allas, Nucl. Phys. **A93**, 31 (1967).

[5]J. R. Calarco, P. M. Kurjan, G. A. Fisher, and S. S. Hanna, Phys. Lett. **92B**, 67 (1980).

[6]L. W. Fagg, Rev. Mod. Phys. **47**, 683 (1975).

[7]T. R. Wang, W. Haeberli, S. W. Wissink, and S. S. Hanna, Phys. Rev. C **37**, 2301 (1988), this issue.

[8]H. F. Glavish, in *Polarization Phenomena in Nuclear Reactions,* Proceedings of the Third International Symposium, Madison, 1970, edited by H. H. Barschall and W. Haeberli (University of Wisconsin Press, Madison, 1971), p. 267.

[9]M. Suffert, W. Feldman, J. Mahieux, and S. S. Hanna, Nucl. Instrum. Methods **63**, 1 (1968).

[10]S. J. Moss and W. Haeberli, Nucl. Phys. **72**, 417 (1965).

[11]P. D. Allen, E. G. Muirhead, and D. V. Webb, Nucl. Phys. **A357**, 171 (1981).

[12]W. R. Dodge and W. C. Barber, Phys. Rev. **127**, 1746 (1962); P. Szalata, K. Itoh, G. A. Peterson, J. Flanz, S. P. Fivozinsky, F. J. Kline, J. W. Lightbody, X. K. Muruyama, and S. Penner, Phys. Rev. C **17**, 435 (1978).

[13]P. P. Singh, R. E. Segel, L. Meyer-Schützmeister, and S. S. Hanna, Nucl. Phys. **65**, 577 (1965).
[14]G. A. Fisher, P. Paul, F. Riess, and S. S. Hanna, Phys. Rev. C **14**, 28 (1976).
[15]H. Feshbach, Ann. Phys. (N.Y.) **5**, 357 (1958); **19**, 287 (1962); H. Feshbach, A. K. Kerman, and R. H. Lemmer, *ibid.* **41**, 230 (1967).
[16]C. M. Shakin and W. L. Wang, Phys. Rev. Lett. **26**, 902 (1971); W. L. Wang and C. M. Shakin, Phys. Rev. C **9**, 2144 (1974).
[17]D. G. Mavis, Ph.D. thesis, Stanford University, 1977.
[18]Y. Gillet, M. A. Melkanoff, and J. Raynall, Nucl. Phys. **A97**, 631 (1967).
[19]J. R. Calarco, S. W. Wissink, M. Sasao, K. Wienhard, and S. S. Hanna, Phys. Rev. Lett. **39**, 925 (1977).
[20]S. W. Wissink, Ph. D. thesis, Stanford University, 1986.
[21]J. L. Black, W. J. O'Connell, S. S. Hanna, and G. L. Latshaw, Phys. Lett. **25B**, 405 (1967).
[22]K. W. Schmid and G. Do Dang, Phys. Lett. **66B**, 5 (1977); Phys. Rev. C **15**, 1515 (1977); **18**, 1003 (1978); K. W. Schmid *ibid.* **24**, 1283 (1981).
[23]R. G. Allas, S. S. Hanna, L. Meyer-Schützmeister, R. E. Segel, P. P. Singh, and Z. Vager, Phys. Rev. Lett. **13**, 628 (1964).